The role of midlatitude storms on air-sea exchange of CO_2

William Perrie,[1,2] Weiqing Zhang,[1,2] Xuejuan Ren,[1,3] Zhenxia Long,[1,2] and Jeff Hare[4,5]

Received 3 December 2003; accepted 12 April 2004; published 5 May 2004.

[1] Hurricanes influence the local rates of air-sea CO_2 exchange. Changes in fCO_{2w}, the fugacity of CO_2 in bulk water, result from storm-induced sea surface temperature (SST) changes and from upwelling. Using numerical studies and comparing recent formulations for the gas transfer velocity k_L, we discuss the impact of Hurricane Gustav (2002) on fCO_{2w} and air-sea CO_2 exchange. We show that Gustav resulted in enhanced CO_2 flux, with the maximum occurring at the storm's peak intensity. *INDEX TERMS:* 0312 Atmospheric Composition and Structure: Air/sea constituent fluxes (3339, 4504); 4504 Oceanography: Physical: Air/sea interactions (0312). **Citation:** Perrie, W., W. Zhang, X. Ren, Z. Long, and J. Hare (2004), The role of midlatitude storms on air-sea exchange of CO_2, *Geophys. Res. Lett.*, *31*, L09306, doi:10.1029/2003GL019212.

1. Introduction

[2] Although the effect of hurricanes on the thermal and physical structure of the upper ocean is relatively well known, their impact on air-sea CO_2 transfer is still emerging. Air-sea gas transfer includes processes such as upper ocean temperature changes and upwelling of carbon-rich deep water. Data sets are few. In the sub-tropical North Pacific, *Kawahata et al.* [2001] report that Hurricane John (1994) caused a 20 μatm fCO_{2w} decrease, upwelling and 2°C SST depression. In the sub-tropical North Atlantic, *Bates et al.* [1998] studied Hurricane Felix (1995), reporting a 60 μatm fCO_{2w} decrease, upwelling, and 4°C SST depression.

[3] Here, we examine the influence of extratropical Hurricane Gustav on air-sea CO_2 exchange in the North Atlantic. This is a CO_2 source region, in terms of annual air-sea flux [*Takahashi et al.*, 2002]. Gustav was selected because it passed 120 km south of the NOAA Ship Ronald H. Brown (hereinafter referred to as Ron Brown) which recorded fCO_{2w} and fCO_{2a}, (fugacity of CO_2 in bulk air) for the Ocean-Atmosphere Carbon Exchange Study (OACES, http://www.aoml.noaa.gov/ocd/gcc/index.php). We describe our model simulation of Gustav in section 2. We present four k_L formulations, and give their U_{10} (wind speed at 10 m height) variation in section 3. These are by *Wanninkhof* [1992], *Wanninkhof and McGillis* [1999], *Zhao et al.* [2003]], and *Fairall et al.* [2000]. Our Gustav simulation allows estimation of the impact of Gustav on the k_L s, and on the CO_2 air-sea flux at the Ron Brown, in section 4.

2. Hurricane Gustav

[4] Gustav propagated by Cape Hatteras on 10 September embedded within a southwesterly flow from a baroclinic cyclogenesis over New England, began intensifying over 28°C Gulf Stream waters and merged with the low, dominated by baroclinic processes. It became a hurricane near 12 UT 11 September, reaching maximum intensity of 42 m/s by 18 UT, and made landfall over Cape Breton at about 06 UT 12 September. Transitioning to an extratropical cyclone, it made a second landfall over Newfoundland.

[5] Gustav influenced the CO_2 exchange (Figure 1). However, no fCO_{2w} data was collected when the storm center passed near the Ron Brown because of high seastate. Thus, we estimate fCO_{2w} as increasing linearly from 377 μatm on 06 UT 11 September until the time of Gustav's peak, and we assume it remains constant at 387 μatm until 14 UT 12 September, following *Bates et al.* [1998]. After the storm passed (after 00 UT 13 Sept.), fCO_{2w} and SST oscillated strongly, reflecting the Gulf Stream environment through which the Ron Brown was moving. Minor oscillations in fCO_{2a} result from sea level pressure (SLP) variations.

[6] Our simulation of Gustav's impact on the CO_2 exchange depends on a reliable model storm simulation. Figures 2a–2b show that Gustav's storm track from our 'full-coupled' atmosphere-ocean model (Appendix A) [*Perrie et al.*, 2004], agrees well with the NHC (National Hurricane Center) storm track and maximum U_{10} verifies well with QSCAT/NCEP (http://dss.ucar.edu/datasets/ds744.4) data. Further verification is given in Figures 3a–3b, for U_{10} and SLP, at NDBC (National Data Buoy Center) buoy 44011 (noted in Figure 1a).

[7] Figures 4a–4b show model estimates for storm-enhanced vertical velocity *w*, SST and temperatures, as functions of time and depth, area-averaged over (71.5°W–73.5°W, 38.5°N–40.5°N), encompassing the Ron Brown's ship track. These variables follow weak oscillatory patterns, with respective magnitudes of 0.0001 m/s for *w*, and 2–3°C for SST depression, because this area is on the left of storm track, and rather distant from the area of Gustav's maximum intensity. SST peaks and upwelling occur in approximate phase, suggesting that both contribute to fCO_{2w} enhancement. This differs from areas of significant SST cooling and upwelling that occur to the right of the

[1]Fisheries and Oceans Canada, Bedford Institute of Oceanography, Dartmouth, Canada.
[2]Department of Engineering Mathematics, Dalhousie University, Halifax, Canada.
[3]Department of Atmospheric Sciences, Nanjing University, Nanjing, China.
[4]CIRES, University of Colorado, Boulder, Colorado, USA.
[5]NOAA ETL, Boulder, Colorado, USA.

0094-8276/04/2003GL019212$05.00

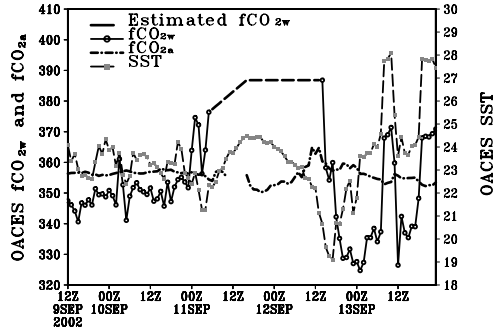

Figure 1. Time series of observed $fCO2_w$, $fCO2_a$, SST (°C), and estimated fCO_{2w} (- - -).

Gustav's storm track where the storm intensity is strong [*Perrie et al.*, 2004].

3. Air-Sea Gas Transfer Velocity

[8] Using variables provided by our coupled model simulation, we estimate the gas transfer velocity k_L. The air-sea CO_2 flux may be written as,

$$Q = k_L \alpha \Delta fCO_2 \tag{1}$$

where α is the solubility of CO_2 and ΔfCO_2 is the difference between fCO_{2w} and fCO_{2a}. Units for Q are mmol $CO_2/m^2/h$. The simplest k_L relations are due to *Wanninkhof* [1992] (hereinafter referred to as Wanninkhof 92) and *Wanninkhof and McGillis* [1999] (hereinafter referred to as Wanninkhof 99),

$$k_L = 0.31\ U_{10}^2 (S_c/660)^{-1/2} \tag{2}$$

$$k_L = 0.0283\ U_{10}^3 (S_c/660)^{-1/2} \tag{3}$$

in terms of U_{10} and the Schmidt number S_c. Units for k_L are cm/h. Additional factors involve wave-breaking and bubbles, as given by *Zhao et al.* [2003] (hereinafter referred to as Toba-Zhao), using a wave-breaking parameter R_B, and the wave spectrum's peak frequency ω_p

$$k_L = 0.13\ R_B^{0.63} \quad \text{and} \quad R_B = u_*^2/\upsilon\omega_p \tag{4}$$

where u_* is the air-side friction velocity, and υ is the kinematic viscosity.

[9] A fourth k_L relation relies on matched water and air fluxes, turbulent and radiative fluxes, U_{10}, sea-state, currents, SST, whitecap fraction *f*, and near-surface thermal structure, as given by *Fairall et al.* [2000] (hereinafter referred to as Fairall)

$$k_L = k_{L(bulk)} + k_{breaking} \tag{5}$$

where the wave-breaking term $k_{breaking}$ [*Woolf*, 1997] is

$$k_{breaking} = f\mathbf{V}\alpha^{-1}\left[1 + \left(\boldsymbol{e}\alpha S_c^{-1/2}\right)^{-1/n}\right]^{-n}; \tag{6}$$

in terms of whitecapping fraction [*Monahan and Torgeresen*, 1991],

$$f = 3.8 \times 10^{-6}\, U_{10}^{\beta}; \quad \beta \approx 3.4. \tag{7}$$

α is the gas solubility and **V**, ***e*** and *n* are empirical constants from the GasEx-1998 field experiment (described by *Fairall et al.* [2000]), respectively 14, 1.2 and 4900 cm/h, and may

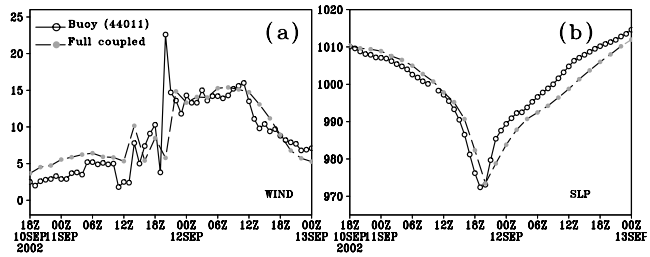

Figure 3. Buoy 44011 (66.59°W, 41.09°N) observations and model simulations for (a) U_{10} (m s^{-1}), and (b) central SLP (mb).

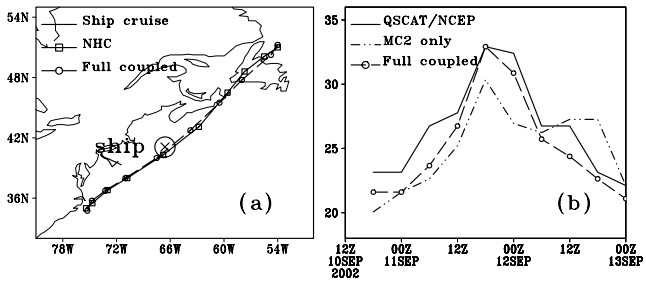

Figure 2. Simulations by the uncoupled MC2 model (- - -), full-coupled model (—○), NHC analysis (—□) and QSCAT/NCEP data (—), for (a) storm track and (b) peak U_{10} (m/s) following the storm center, beginning at 18 UT 10 September. Buoy station 44011 is ⊗.

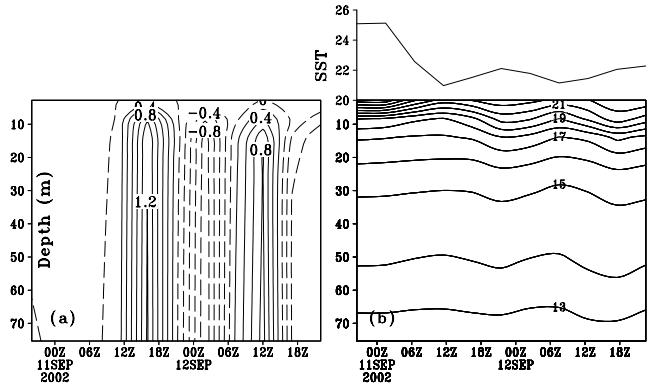

Figure 4. Model estimates for (a) Vertical velocity ($\times 10^{-4}$m/s) *w*, and (b) temperature (°C), averaged over the area 71.5°W–73.5°W and 38.5°N–40.5°N, encompassing the Ron Brown, as a function of depth and time. SST is included in (b). Positive *w* is upward.

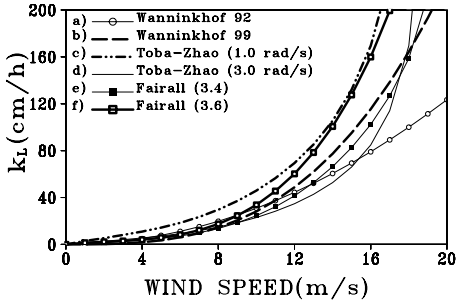

Figure 5. Gas transfer velocities k_L as a function of U_{10} from: (a) Wanninkhof 92, (b) Wanninkhof 99, (c) Toba-Zhao with ω_p = 1 rad/s, and (d) with ω_p = 3 rad/s, (e) Fairall with β = 3.4, and (f) with β = 3.6.

need re-adjustment for other data-sets, although their determination is an ongoing topic of research [*Hare et al.*, 2004]. The interfacial term $k_{L(bulk)}$ is

$$k_{L(bulk)} = \frac{u_*}{\sqrt{\rho_w/\rho_a}\left(h_w S_{cw}^{1/2} + \ln(z_w/\delta_w)/\kappa\right) + \alpha\left(h_a S_{ca}^{1/2} + C_d^{-1/2} - 5 + \ln(S_{ca})/(2\kappa)\right)} \quad (8)$$

where subscript "a" ("w") denotes air- (water-)side, ρ is density, z is the measurement depth, δ is the turbulent surface layer thickness, κ is the von Kármán constant, C_d is the drag coefficient, and h is defined by $h \equiv \Lambda R_r^{1/4}/\varphi$, where Λ is an adjustable constant, R_r is the roughness Reynolds number, and φ is an empirical function that accounts for buoyancy effects on turbulent transfer in the ocean. Variables u*, C_d, and R_r come from the Toga-COARE bulk flux parameterizations [*Fairall et al.*, 2003]. The Schmidt number in air S_{ca} is from *Fairall et al.* [2000, Table 1].

[10] Figure 5 compares the k_L s in equations (2)–(7), assuming no surface currents or rain, SST is 20°C, screen temperature (at 2 m) T_a is 18.2°C, water specific humidity is 18.0 g/kg, air specific humidity is 15.5 g/kg, downward solar flux and infrared flux are 141.0 W/m^2 and 419.0 W/m^2 respectively, peak frequency is 3 s and 1 s, wave-height is 1 m, and salinity is 35%. Thus, for $U_{10} > 12$ m/s, differences in the k_L curves increase rapidly. Wanninkhof 92's k_L relation is the lowest of all, and the other 3 k_L s can be similar (with $\omega_p = 3\ s^{-1}$).

[11] The Fairall and Toba-Zhao formulations are very sensitive to changes in β and ω_p, respectively, and probably represent the upper bounds on k_L. Increasing β slightly from 3.4 to 3.6, or decreasing ω_p from 1 s^{-1} to 3 s^{-1}, results in large k_L changes compared to other k_L curves. Furthermore, as whitecap coverage data are extremely noisy, this variation in β does not begin to capture the variability in the field data, particularly at high-wind speeds where there is very little data. In fact β should depend on U_{10} and seastate variables. Moreover, the Toba-Zhao k_L was calibrated with freshwater data where whitecaps were generated by waves shoaling, which can differ significantly with whitecap-related CO_2 transfer in seawater [*Asher et al.*, 1997].

4. Gas Transfer Velocity and CO_2 Air-Sea Flux

[12] Using variables from our Gustav simulation, Figure 6 compares the k_L s at the Ron Brown location. All k_L formulations follow similar trends, showing the storm's impact. As in Figure 5, the Wanninkhof 92 relation is lower than the other three, at Gustav's peak. The Toba-Zhao and Wanninkhof 99 relations are close, except for variations due to wave effects (R_B and ω_p) when U_{10} is moderate. Fairall's k_L is the highest of the four relations (assuming β = 3.4), particularly at Gustav's peak.

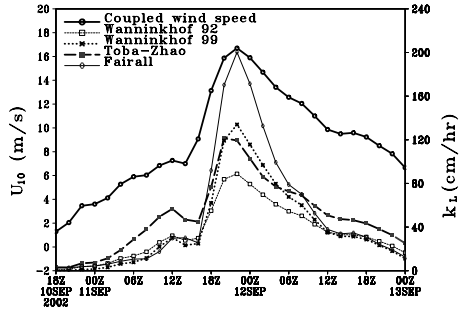

Figure 6. Time series of U_{10} comparing k_L formulations, averaged over area (71.5°W–73.5°W, 38.5°N–40.5°N), encompassing the Ron Brown.

[13] At Gustav's peak (18 UT 11 Sept.), k_L distributions for the North Atlantic are shown in Figure 7. Wanninkhof 92's k_L is the lowest, and although the Toba-Zhao k_L and Wanninkhof 99 k_L are similar, the former exhibits extensive variability over the ocean, reflecting wave impacts. By comparison, the other three k_L relations show less variability and are significant for local areas near the storm center. Fairall's k_L has higher values than the other three, more than twice those of Wanninkhof 92's k_L.

[14] Using the four k_L models, and observed and estimated fCO_{2w} and fCO_{2a} data at the Ron Brown, Figure 8 presents the net air-sea CO_2 flux Q. Solubility α is computed from the observed SST and salinity, and Q was area-averaged over (71.5°W–73.5°W, 38.5°N–40.5°N) around the Ron Brown. Trends in Q reflect k_L trends in Figures 6–7. Before Gustav's passage, Q is almost zero. Within hours of Gustav's passing, Q increases to a maximum out-flux of

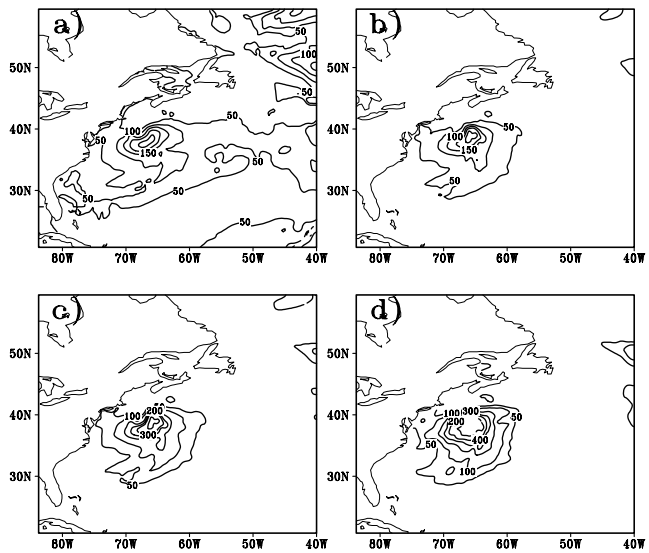

Figure 7. k_L at Gustav's peak (18 UT 11 Sept.) from (a) Toba-Zhao, (b) Wanninkhof 92, (c) Wanninkhof 99, and (d) Fairall. Units are cm h^{-1}.

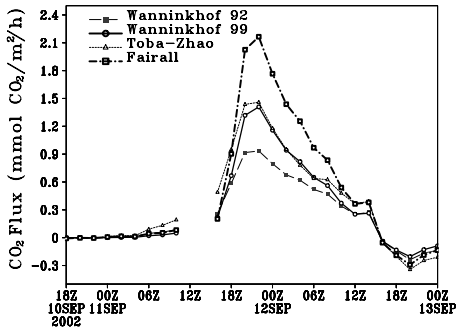

Figure 8. Time series of CO_2 flux Q, using four k_L s, averaged over (71.5°W–73.5°W, 38.5°N–40.5°N) around the Ron Brown. The gap at 12 UT occurs because no fCO_{2a} data is available.

2.1 mmol/m^2/h (Fairall's k_L), decreases to zero within 18 h, and briefly to −0.4 mmol/m^2/h, thereafter.

5. Summary

[15] We used OACES data to estimate the impact of Hurricane Gustav on air-sea CO_2 exchange, comparing four recent k_L relations. In high winds, the Wanninkhof 92 k_L is the lowest of these relations. The Toba-Zhao and Wanninkhof 99 k_L s are close to one another, although the former has extensive variability over the ocean due to the wave effects, while the other three relations are significant over local areas near the storm center. During Gustav's peak, Fairall's k_L is the highest, more than twice Wanninkhof 92's, due to white-capping. Fairall's k_L, and Toba-Zhao's, are sensitive to whitecap coverage, and peak frequency, respectively.

[16] Based on interpolated fCO_{2w} data, Gustav caused a rapid increase in CO_2 out-flux, reaching a maximum of 2.1 mmol/m^2/h (assuming Fairall's k_L) occurring at the storm's peak and diminishing rapidly to zero within 18 h later. However, this k_L is tuned to Gas-Ex data and may need adjustment for other environmental conditions [*Hare et al.*, 2004].

Appendix A

[17] The model couples atmosphere and ocean components, passing fluxes of heat, momentum and mass. The atmospheric model is MC2 [*Benoit et al.*, 1997], implemented at 0.25° resolution, with 30 vertical layers, and 600s time steps. Boundary and initial conditions are from Canadian Meteorological Centre analysis data. The ocean model is POM (Princeton Ocean Model) by G. L. Mellor (http://splash.princeton.edu/WWWPUBLIC/htdocs.pom) with 0.16° horizontal resolution, 23 vertical layers. Boundary and initial conditions are from the Generalized Digital Environmental Model (GDEM) data [*Bender and Ginis*, 2000]. The wave model is WAVEWATCH III. The sea spray model simulates total air-sea latent and sensible heat fluxes [*Andreas and DeCosmo*, 2002].

[18] **Acknowledgments.** We acknowledge funding from the Canada Panel on Energy Research and Development and Natural Science and Engineering Research Council (SOLAS), and assistance with the MC2 model (J. Gyakum, R. McTaggart-Cowan), the sea spray model (E. Andreas), the URI POM version (I. Ginis), and the fourth k_L model (C. Fairall).

References

Andreas, E. L., and J. DeCosmo (2002), The signature of sea spray in the HEXOS turbulent heat flux data, *Boundary Layer Meteorol.*, *103*, 303–333.

Asher, W. E., L. M. Karle, and B. J. Higgins (1997), On the differences between bubble-mediated air-water transfer in freshwater and seawater, *J. Mar. Res.*, *55*, 813–845.

Bates, N. R., A. H. Knap, and A. F. Michaels (1998), Contribution of hurricanes to local and global estimates of air-sea exchange of CO_2, *Nature*, *395*, 58–61.

Bender, M. A., and I. Ginis (2000), Real-case simulations of hurricane-ocean interaction using a high-resolution coupled model: Effects on hurricane intensity, *Mon. Weather Rev.*, *128*, 917–946.

Benoit, R., M. Desgagne, P. Pellerin, Y. Chartier, and S. Desjardins (1997), The Canadian MC2: A semi-implicit semi-Lagrangian wide-band atmospheric model suited for fine-scale process studies and simulation, *Mon. Weather Rev.*, *125*, 2382–2415.

Fairall, C. W., J. E. Hare, J. B. Edson, and W. McGillis (2000), Parameterization and micro-meteorological measurements of air-sea gas transfer, *Boundary Layer Meteorol.*, *96*, 63–105.

Fairall, C. W., E. F. Bradley, J. E. Hare et al. (2003), Bulk parameterization of air-sea fluxes: Updates and verification for the COARE algorithm, *J. Clim.*, *16*, 571–591.

Hare, J. E., C. W. Fairall, W. R. McGillis et al. (2004), Evaluation of the National Oceanic and Atmospheric Administration/Coupled-Ocean Atmospheric Response Experiment (NOAA/COARE) air-sea gas transfer parameterization using GasEx data, *J. Geophys. Res.*, *109*, doi:10.1029/2003JC001831, in press.

Kawahata, H., A. Suzuki, L. P. Gupta, and H. Ohta (2001), Decrease in the CO_2 fugacity during a hurricane event, paper presented at the 6th International Carbon Dioxide Conference, Tohoku Univ., Sendai, Japan.

Monahan, E. C., and T. Torgeresen (1991), The enhancement of air-sea gas exchange by oceanic whitecapping, in *Air-Water Mass Transfer: Proceedings of the 2nd International Symposium on Gas Transfer at Water Surfaces*, edited by S. C. Wilhelms and J. S. Gulliver, pp. 608–617, Am. Soc. of Chem. Eng., New York.

Perrie, W., X. Ren, W. Zhang, and Z. Long (2004), Simulation of extatropical Hurricane Gustav using a coupled atmosphere-ocean-sea spray model, *Geophys. Res. Lett.*, *31*, L03110, doi:10.1029/2003GL018571.

Takahashi, T., S. Sutherland, C. Sweeney et al. (2002), Global sea-air CO_2 flux based on climatological surface ocean pCO_2 and seasonal biological and temperature effects, *Deep Sea Res., Part II*, *49*, 1601–1622.

Wanninkhof, R. (1992), Relationship between wind speed and gas transfer exchange over the ocean, *J. Geophys. Res.*, *97*, 7373–7382.

Wanninkhof, R., and W. R. McGillis (1999), A cubic relationship between air-sea CO_2 exchange and wind speed, *Geophys. Res. Lett.*, *26*, 1889–1892.

Woolf, D. K. (1997), Bubbles and their role in gas exchange, in *The Sea Surface and Global Change*, edited by R. A. Duce and P. S. Liss, pp. 173–205, Cambridge Univ. Press, New York.

Zhao, D., Y. Toba, Y. Suzuki, and S. Komori (2003), Effect of wind waves on air-sea gas transfer: Proposal of an overall CO_2 transfer velocity formula as a function of breaking-wave parameter, *Tellus, Ser. B*, *55*, 478–487.

Z. Long, W. Perrie, X. Ren, and W. Zhang, Fisheries and Oceans Canada, Bedford Institute of Oceanography, P.O. Box 1006, 1 Challenger Drive, Dartmouth, NS, Canada B2Y 4A2. (perriew@dfo-mpo.gc.ca)

J. Hare, CIRES, University of Colorado, 216 UCB, Boulder, CO 80309, USA.